Identified Particle Spectra and Jet Interactions with the Medium

P. Sorensen[a]

[a]Brookhaven National Laboratory, Upton, New York 11973-5000, USA

Through a combination of detector upgrades and advancements in analysis techniques, physicist at RHIC are extending their ability to identify particles at high p_T. With these new capabilities some outstanding questions are being addressed: particularly regarding baryon production. Here I present an overview of new data on identified particle elliptic flow (v_2), identified particle p_T spectra and identified hadron-hadron correlations. The observed phenomena provide insights into hard parton interactions with the bulk matter created in heavy-ion collisions and the relevant degrees-of-freedom during its early stages.

1. Introduction

Physicists at the Relativistic Heavy Ion Collider (RHIC) have made several unexpected observations [1]. Of particular interest are measurements relating to baryon production in the intermediate transverse momentum region ($1.5 < p_T < 5$ GeV/c) [2–4]. In nucleon-nucleon collisions at $p_T = 3$ GeV/c, one baryon is produced for every three mesons (1:3). In $Au+Au$ collisions however, baryons and mesons are created in nearly equal proportion (1:1). At this same p_T, the elliptic anisotropy (v_2) of baryons is also 50% larger than meson elliptic flow: demonstrating that baryon production is also enhanced in the direction of the impact vector between the colliding nuclei (in-plane) [3,5]. This enhancement in baryon production persists up to $p_T = 5.5$ GeV/c. Several possible explanations for the enhancement are commonly considered:

> Multi-quark or gluon processes during hadron formation—*coalescence* [6].
>
> Gluon configurations that carry baryon number—*baryon junctions* [7,8].
>
> Collective motion amongst more massive baryons that populates the higher p_T regions of baryon p_T spectra—*flow* [9].

Coalescence models have garnered particular attention because they seem to provide a natural explanation for the constituent-quark-number scaling that has been observed in v_2 measurements. They also relate hadronic observables to a pre-hadronic stage of interacting quarks and gluons. As such, they touch on questions central to the heavy-ion physics program: deconfinement and chiral symmetry restoration.

Given the potential physics benefits that can be derived from these measurements, RHIC physicists have endeavored to extend their abilities to identify hadron types up to higher p_T regions [10,11]. Through these efforts, measurements of $\pi^{\pm}$, π^0, K^0_S, η, $p+\overline{p}$, and $\Lambda+\overline{\Lambda}$ spectra and v_2 which extend beyond $p_T = 8$ GeV/c have been presented at

this conference. Here I review those measurements along with correlation measurements that may help clarify some of the questions remaining about the origin and implications of the baryon enhancement in heavy-ion collisions.

1.1. Azimuthal Dependence: v_2

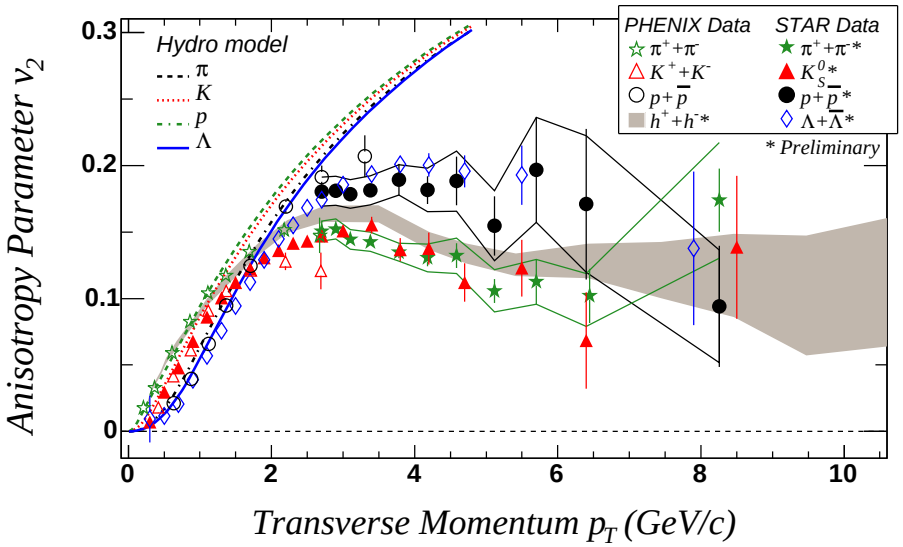

Figure 1. Elliptic flow measurements at middle rapidity from minimum-bias $Au + Au$ collisions at $\sqrt{s_{NN}} = 200$ GeV. The bands around the STAR preliminary measurments of pions and protons represent systematic uncertainties mostly from non-flow correlations. The PHENIX measurements are made by correlating hadrons at middle rapdity with an event-plane measured using hadrons at $3.1 < |\eta| < 4.0$. For this reason they are less susceptible to most spurious, non-flow correlations.

Fig. 1 shows preliminary measurements of v_2 with a minimum bias centrality selection in $Au + Au$ collisions at $\sqrt{s_{NN}} = 200$ GeV/c [12,13]. The curves show v_2 for pions, kaons, protons and Lambdas from a hydrodynamic calculation [9]. At $p_T < 1.0$ GeV/c, the mass ordering observed demonstrates that v_2 in that region results from collective motion and the hydrodynamic calculations capture the general features of the data in this region. At much higher p_T it is expected that v_2 will be developed via energy loss by fast partons as they traverse the medium created in the collisions. Calculations suggest that v_2 from this mechanism should be less than 10% [14]. It is also expected that all hadrons will have similar v_2 values where energy loss mechanisms dominate v_2. The magnitude and particle-type dependence of v_2 seen for $p_T < 6$ GeV/c suggest that other mechanisms contribute to the developement of v_2 up to 6–7 Gev/c. This observation is consistant with results from a parton cascade model predicting that the effects of flow may persist up to $p_T = 7$ GeV/c [15]. At $p_T = 7$ GeV/c, where, within errors, the particle-type dependence of v_2 dissappears, the v_2 measurements are consistant with expectations from energy loss models [14].

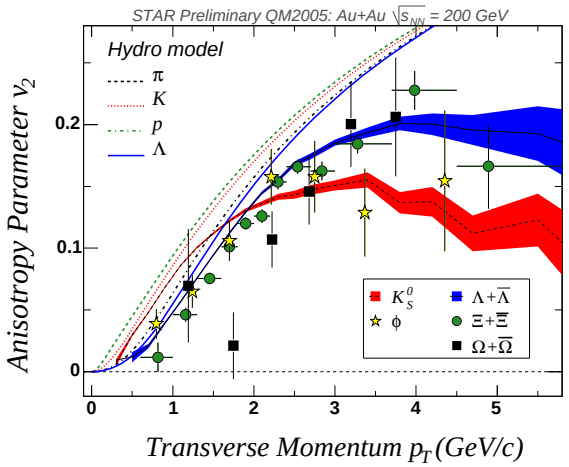

Figure 2. Preliminary measurements of strange hadron elliptic flow shown by the STAR collaboration at QM2005. The measurements are made at middle-rapidity with a minimum-bias centrality selection corresponding to 0%–80% of the hadronic cross-section. Only statistical errors are shown. Curves are hydrodynamic model calculations [9].

Multi-strange hadron v_2 measurements with unprecedented accuracy were presented at this conference [12]. These measurements are thought to be good tests for collective effects amongst quarks and gluons [16]. Measurements show that when the p_T spectra of ϕ-mesons and Ω-baryons are characterized with a two component hydrodynamic inspired fit, the temperature and flow velocity parameters extracted are systematically different than those extracted for non-strange hadrons [1]. The differences are consistent with less hadronic rescattering amongst multi-strange hadrons. For this reason, it is believed that the v_2 of multi-strange hadrons reflects collectivity that developed before hadrons formed.

In Fig. 1.1 v_2 measurements for K^0_S, ϕ, $\Lambda + \overline{\Lambda}$, $\Xi + \overline{\Xi}$, and $\Omega + \overline{\Omega}$ from minimum bias $Au + Au$ collisions at $\sqrt{s_{NN}} = 200$ GeV are shown. The ϕ and Ω v_2 values follow the same systematic trends as the non-strange hadrons: with an apparent mass ordering at low p_T and a quark-number dependence at intermediate p_T. Combined with the spectra measurements, these measurements suggests that v_2 is developed during a prehadronic stage.

1.2. Quark Number Dependence

Hadronization by coalescence or recombination of constituent quarks is thought to explain many features of hadron production in the intermediate p_T region ($1.5 < p_T < 5$ GeV/c) [6]. These models find that at intermediate p_T, v_2 may follow a quark-number (n_q) scaling with $v_2(p_T/n_q)/n_q$ for all hadrons falling on one curve. This scaling behavior has been observed in $Au + Au$ collisions at 200 GeV [5]. More sophisticated theoretical considerations have led to predictions of fine structure in quark-number scaling, with predictions for a baryon v_2/n_q being smaller than meson v_2/n_q [17,18].

Fig. 1.2 (top panel) shows v_2 vs p_T for identified particles, where v_2 and p_T have been scaled by n_q. A polynomial function is fit to the scaled values. The deviations from the scaling are shown in the bottom panel by plotting the difference between the scaled baryon v_2 and the scaled meson v_2 divided by the sum $(B - M)/(B + M)$. Theoretical predictions for this value are also shown. The model that compares best to data is a coalescence model that includes the effect of quark momentum distributions inside the hadron (*Coalescence + wavefunction*) [17]. The effect of accounting for the substructure of constituent quarks (*higher fock states*) [18] leads to a negative $(B - M)/(B + M)$ ratio

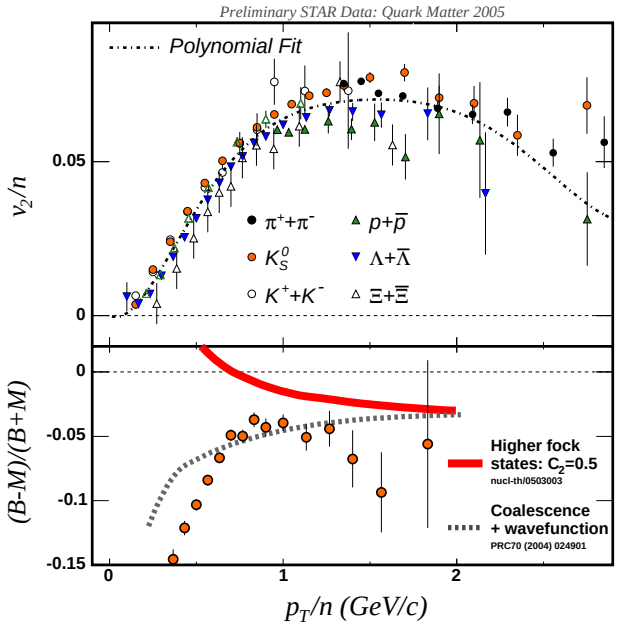

Figure 3. Top panel: Quark number scaled elliptic flow for identified hadrons. A polynomial is fit to all data points. Bottom panel. The difference between quark number scaled baryon v_2 and quark number scaled meson v_2 divided by the sum: $(B-M)/(B+M)$. Here the ratio is taken using hyperons and kaons). The solid curve shows model predictions when the daughter partons of the constituent quarks are considered. The dashed line shows model results after the momentum distributions of the constituent quarks are taken into account.

but with a smaller magnitude than observed in the data. It should be noted, however, that the systematic uncertainties on the measurements have not yet been estimated.

Quark-number dependences at intermediate p_T are also manifested in the centrality dependence of the p_T spectra. Fig. 4 shows the ratios R_{CP} [3,19–21] (central $Au+Au$ over peripheral $Au+Au$ in the left panel) and R_{AA} [22,23] ($Au+Au$ over $p+p$ in the right panel) where the spectra have been scaled by the number of binary nucleon-nucleon collisions (N_{bin}) to account for trivial increase in yields with system size. Hard processes are expected to scale with N_{bin}, so $R_{AA,CP} < 1$ at high p_T indicates a suppression due to nuclear affects. Models incorporating energy loss of hard scattered partons in medium successfully describe the suppression of hadrons at high p_T [14]. Indeed, photons which only interact electro-magnetically are found to follow N_{bin} scaling. Here, however we concentrate on the features of the particle-type dependence of hadrons at intermediate p_T.

For $p_T > 1.5$ GeV/c, R_{CP} values are grouped by particle type (mesons vs. baryons). The larger baryon R_{CP} values indicate that baryon production increases more quickly with centrality than meson production. This observation is confirmed with good precision for protons and hyperons. The ϕ is a particularly interesting test particle since it is a meson but is more massive than the proton. With good precision, the ϕ is now confirmed to follow the systematics of the other mesons. Additionally R_{AA} has been measured for the η-meson and its values are similar to those of the pions.

Particular progress has been made in the measurement of charged pion and proton R_{CP}. These measurements now extend into the region where fragmentation in vacuum is thought to be the dominate hadronization mechanism. In this region, if the relative fraction of quark and gluon jets (fragmenting to a hadron with a given p_T) changes from peripheral to central $Au+Au$ collisions, the R_{CP} of different particle types may take on different values. This is a result of the difference in the shapes of the fragmentation

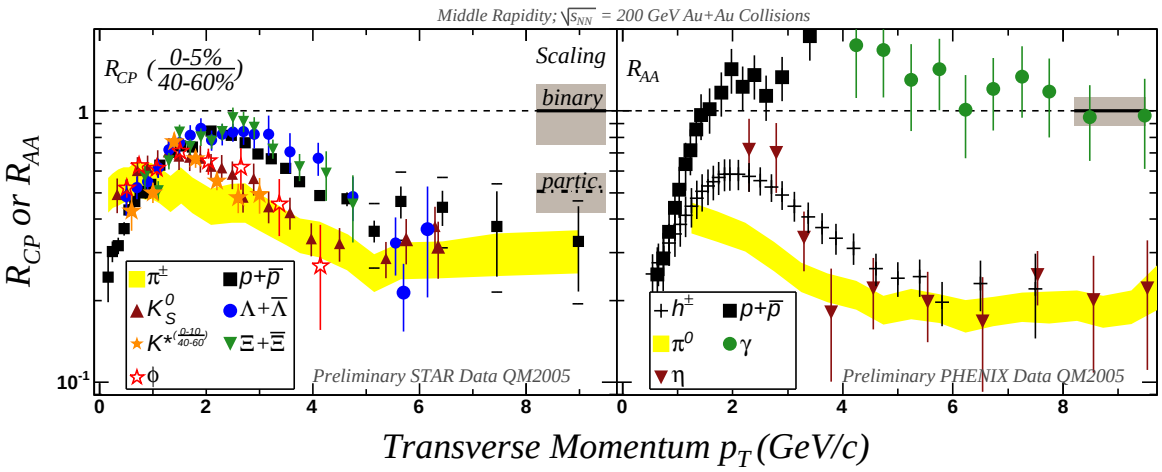

Figure 4. Preliminary identified particle R_{CP} (left panel) and R_{AA} (right panel). Grey bands represent the error on the N_{bin} and N_{part} calculations. For the R_{AA} data, error bars represent both systematic and statistical uncertainties. For pion R_{CP}, the yellow band includes both systematic and statistical uncertainties. For proton R_{CP}, the systematic uncertainties are shown as brackets on the final five points (systematic uncertainties are similar for lower p_T points).

functions of quark and gluon jets. Within errors however, the $\pi^{\pm}$, K^0_S, $p+\overline{p}$, and $\Lambda+\overline{\Lambda}$ R_{CP} values at $p_T = 6.5$ GeV/c appear to be consistent with each other. The systematic errors on the proton R_{CP} still, however, allow for significant deviations between proton and pion R_{CP}.

Measurement of K^0_S and $\Lambda+\overline{\Lambda}$ R_{CP} at $\sqrt{s_{NN}} = 17.2$ GeV indicate that baryon production is also enhanced compared to mesons at lower center-of-mass energies [24]: with $\Lambda+\overline{\Lambda}$ R_{CP} values well above N_{bin} scaling. It has been proposed that the large baryon R_{CP} values at RHIC may be a result of the suppression of meson production coupled with novel baryon production mechanisms scaling with N_{bin} or N_{part} [8]. The lower energy measurements call this interpretation into question since baryon production is still enhanced even while the suppression of mesons is much weaker.

Since the grouping of R_{CP} with quark number appears to be extend across many hadron species, the centrality dependence of intermediate p_T particle yields may provide information about the quark content of non-$q\overline{q}$ candidates. The $f_0(600)$, $f_0(980)$, $a_0(980)$, and $\kappa(800)$ are all candidates for four-quark or $K\overline{K}$-molecular states [25–27]. The branching ratio for $\phi \to \pi^0\pi^0\gamma$ decays, which is sensitive to the structure of the f_0, favors the f_0 as a four-quark state [28]. In Fig. 1.2, a sketch is shown of what R_{CP} may look like for the f_0 if it is a four-quark or $K\overline{K}$-molecular state. $f_0(980)$ R_{CP} can be measured from the $\pi^+\pi^-$ invariant mass spectrum [29]. If at $p_T = 3$ GeV/c its value is similar to other mesons, the f_0 is either a two quark-state or the baryon enhancement is not a function of the number of quarks: strongly favoring baryon junctions as the source of the baryon enhancement. The result that f_0 R_{CP} is greater than the baryon R_{CP}, will strongly favor f_0 as a four-quark or $K\overline{K}$ state and coalescence as the dominant hadronization process for intermediate p_T hadrons. Measurements of the $\pi^+\pi^-$ invariant mass spectrum should

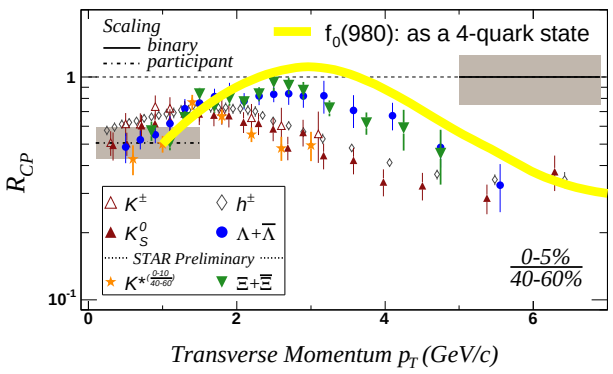

Figure 5. A sketch of what R_{CP} may look like for the $f_0(980)$ meson if it is a non-$q\overline{q}$ state. At p_T = 3 GeV, $f_0(980)$ $R_{CP} > 1$ would favor the $f_0(980)$ as a four-quark or $K\overline{K}$-molecular state. If $f_0(980)$ R_{CP} values are similar to those for other mesons, either the $f_0(980)$ is a two-quark state or coalescence/recombination is not the dominant formation mechanism.

be sensitive to the large difference between these scenarios.

2. Baryon to Meson Ratios

The quark-number scaling of v_2 and the meson vs. baryon grouping of R_{CP} demonstrate the relevance of constituent-quark number. The first indication of these effects came from measurements of the proton-to-pion ratio at RHIC [2]. Fig. 6 (left panel) shows the $\overline{p}/\pi^-$ ratio measured in $e^+ + e^-$ [30], $p+p$ [20], and $Au+Au$ [2,20] collisions. The right panel shows the $\Lambda + /K^0_S$ ratio for $p+p$, mid-peripheral $Au+Au$, and central $Au+Au$ collisions scaled by 0.5 to fit on the same axis. The baryon enhancement at intermediate p_T is pronounced in central $Au+Au$ collisions with $\overline{p}/\pi^-$ reaching a maximum value of nearly 1 at $p_T \approx 3$ GeV/c. The baryon junction calculations in Ref. [8] predict that the p_T value where the B/M ratio is at its maximum will increase with collision centrality. This prediction can be compared to the Λ/K^0_S data. Measurements are still not precise enough, however, to confirm nor disprove this prediction.

Fig. 6 also demonstrates that the baryon enhancement in $Au+Au$ collisions may be part of a systematic trend. Baryon production is also enhanced in $\sqrt{s} = 10$ GeV $e^+ + e^-$ collisions when $e^+e^- \rightarrow \Upsilon \rightarrow ggg$ events are compared to continuum $e^+e^- \rightarrow q\overline{q}$ events [30]. From those measurements the question was posed: *is the enhancement related to multi-parton topological effects or a difference between quark and gluon fragmentation?* Since $e^+e^- \rightarrow \Upsilon \rightarrow ggg$ is a purely gluonic process, the observation that the $\overline{p}/\pi^-$ ratio is even larger in $Au+Au$ collisions indicates that multi-parton topological effects drive the enhancement (baryon junctions or coalescence).

3. Jet interactions with the medium

Also included in the left panel of Fig. 6 are measurements of the $(p+\overline{p})/(\pi^+ + \pi^-)$ ratio in jets observed in $Au+Au$ collisions [31]. The analysis triggers on "high p_T" hadrons ($2.5 < p_T < 4.0$ GeV/c) and measures the proton and pion yields in the peaks observed around the trigger hadron (near-side) and the peak opposite the trigger hadron (away-side). Because of energy-loss, triggering on high p_T hadrons will select events where a hard scattering occurred near the surface of the $Au+Au$ collision overlap region.

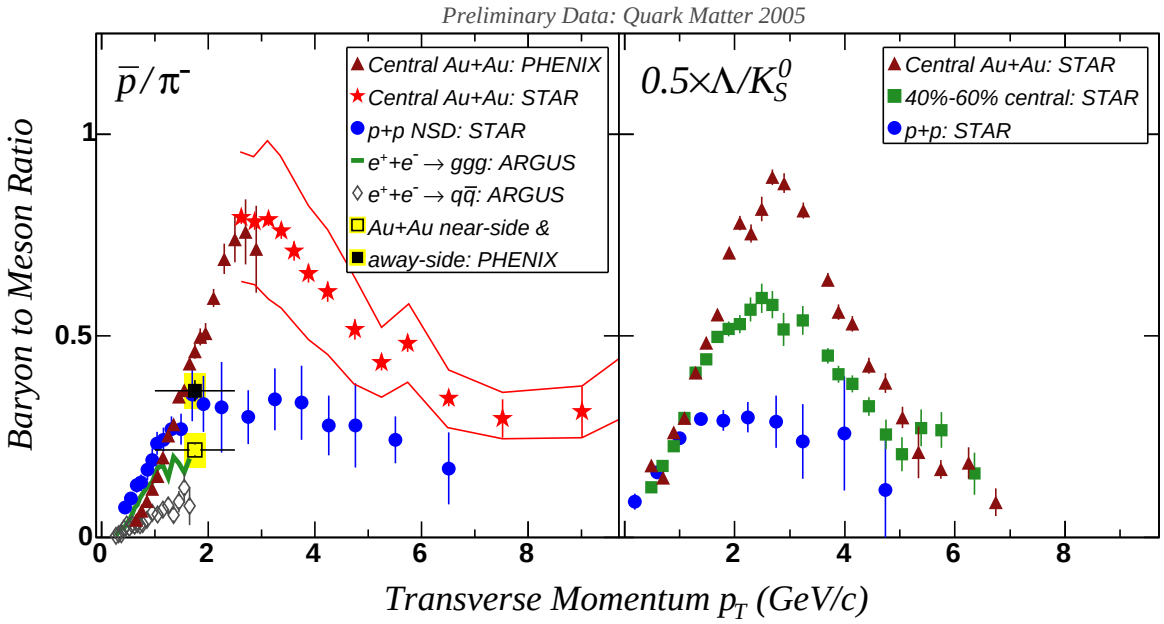

Figure 6. Left panel: the $\overline{p}/\pi^-$ ratio at middle rapidity for central $Au + Au$ and $p + p$ collisions at $\sqrt{s_{NN}} = 200$ GeV. ARGUS measurements of the proton to pion ratio in $e^+ + e^-$ collisions $\sqrt{s} = 10$ GeV are shown for two classes of events: $e^+e^- \rightarrow \Upsilon \rightarrow ggg$ and continuum events dominated by $e^+e^- \rightarrow q\overline{q}$. Measurements of the proton to pion ratio made for particles associated with a trigger hadron ($p_T > 2.5$) are also shown. Left panel: $\Lambda + \overline{\Lambda}/K^0_S$ in central $Au + Au$, mid-peripheral $Au + Au$ and minimum-bias $p + p$ collisions. Values are scaled by 0.5.

In this case, one of the fast partons can escape relatively unperturbed while the other fast parton must traverse the bulk matter created in the $Au + Au$ collision. The near-side baryon-to-meson ratio then should reflect hadron production outside the matter, while the away-side ratio should reflect hadron production within the matter. The result $(p+\overline{p})/(\pi^+ + \pi^-)_{away-side} > (p+\overline{p})/(\pi^+ + \pi^-)_{near-side}$ is then consistent with the baryon enhancement arising from multi-gluon or multi-quark processes in hadron production.

Baryon production may be further favored by the recoil that the matter undergoes in response to an impinging hard parton. Fig. 7 shows measurements of p_T autocorrelations in 20%–30% central, 200 GeV, $Au + Au$ collisions [32,33]. The left panel shows the auto-correlations after subtracting sinusoidal modulations associated with v_2. The remaining features are a positive near-side peak (associated with an escaping hard parton), a negative near-side valley, and a broad, positive, away-side peak. The right panel shows the same data plotted on a cylinder after the positive near-side peak is subtracted. The data show that the p_T distribution of hadrons—close in η and ϕ to an escaping hard parton—is red-shifted. This apparent recoil can lead to collective motion amongst the matters constituents in the direction of the impinging partons momentum. This jet-induced flow will lead to an increase in the number of co-moving constituents on the away-side of an escaping hard parton. The data, in Figs. 1, 4, and 6 show that wherever the density of

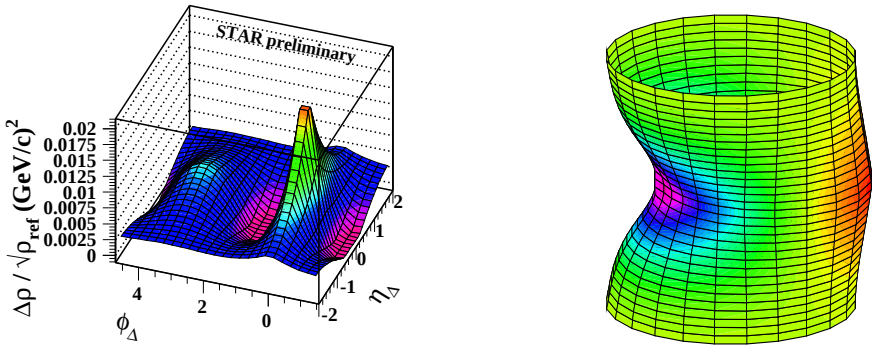

Figure 7. Left panel: p_t autocorrelations derived from the $\langle p_t \rangle$ fluctuation scale dependence in $Au + Au$ collisions at $\sqrt{s_{NN}} = 200$ GeV [32]. Sinusoidal modulations associated with v_2 have been subtracted. Right Panel: p_t autocorrelations plotted in cylindrical coordinates. The positive *near-side* mini-jet peak is subtracted. The figure demonstrates that the medium in $Au + Au$ collisions recoils in response to an impinging parton [33].

co-moving constituents is larger, baryon production is enhanced. Now the near-side, and away-side data in 6 shows that baryon production is also enhanced in the recoil region of quenched jets.

4. Anti-baryon to Baryon Ratios

Further information about baryon production can be gleaned from anti-baryon to baryon ratios ($\overline{B}/B$). Fig. 8 shows $\overline{B}/B$ for protons (left panel) and lambda hyperons (right panel). The curves show model expectations from Ref. [8]. Disagreement between the pQCD calculation and the data are evident and indicate the importance of non-perturbative effects in baryon production at $p_T < 6$ GeV/c. The *Soft+Quench* calculation uses a phenomenological treatment of baryon junctions to successfully predict the observed trends. For this calculation, the apparent baryon enhancement is revealed through the suppression of high-p_T meson production. It is not clear, however, that this model can successfully describe the $\sqrt{s_{NN}}$, and system-size dependence of the $\overline{p}/\pi^-$ ratio: particularly given that baryon production appears to be enhanced in $d+Au$ collisions [34] collisions and $Pb+Pb$ collisions at $\sqrt{s_{NN}} = 17.2$ GeV [24], where little or no high-p_T suppression is seen.

5. Conclusions

Pion, kaon, proton, and hyperon momentum-space distributions have been measured up-to $p_T \approx 10$ GeV/c. Several observations indicate that at $p_T > 6$ GeV/c, hard processes may dominate particle production. Below this, measurements of the B/M ratios, the $\overline{B}/B$ ratios, R_{CP}, and v_2 indicate that processes beyond the reach of perturbative QCD are prevalent. Measurements favor pictures involving either a large contribution from coalescence processes during hadronization or the presence baryon junctions. The systematics of the baryon enhancement—including the $\sqrt{s_{NN}}$ dependence, the collision system dependence (particularly $d+Au$), and the B/M ratios on the near- and away-side

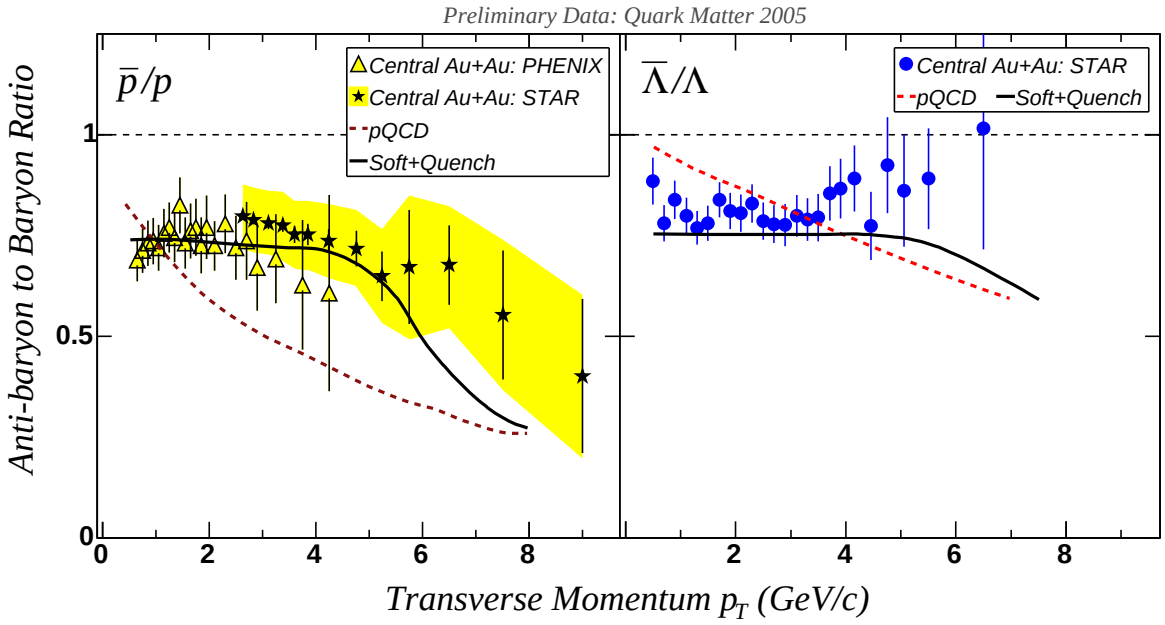

Figure 8. Left panel: $\overline{p}/p$ at middle rapidity from central $Au + Au$ collisions for $\sqrt{s_{NN}} =$ 200 GeV. The yellow band represents the systematic uncertainties on the preliminary STAR measurements. Right panel: Preliminary STAR measurements of $\overline{\Lambda}/\Lambda$ at middle rapidity in central $Au + Au$ collisions at $\sqrt{s_{NN}} = 200$ GeV.

of trigger hadrons—may be a challenge to the baryon junction picture. If the coalescence models are correct, identified particle v_2 measurements imply that a highly interacting quark and gluon phase exists in heavy ion collisions prior to hadron formation. The validity of such a phase is also favored by the large v_2 values observed for multiply strange hadrons.

Acknowledgments: I'd like to thank the conference organizers for the invitation to Budapest, along with H. Huang, H-G. Ritter, and N. Xu for their guidance.

REFERENCES

1. K. Adcox *et al.* [PHENIX Collaboration], Nucl. Phys. A **757**, 184 (2005); J. Adams *et al.* [STAR Collaboration], Nucl. Phys. A **757**, 102 (2005).
2. S. S. Adler *et al.* [PHENIX Collaboration], Phys. Rev. Lett. **91**, 172301 (2003).
3. J. Adams *et al.* [STAR Collaboration], Phys. Rev. Lett. **92**, 052302 (2004).
4. P. R. Sorensen, J. Phys. G **31**, S889 (2005). P. R. Sorensen, arXiv:nucl-ex/0309003.
5. J. Adams *et al.* [STAR Collaboration], Phys. Rev. C **72**, 014904 (2005).
6. D. Molnar and S. A. Voloshin, Phys. Rev. Lett. **91**, 092301 (2003); R. C. Hwa and C. B. Yang, Phys. Rev. C **67**, 064902 (2003); R. J. Fries, B. Muller, C. Nonaka and S. A. Bass, Phys. Rev. C **68**, 044902 (2003); V. Greco, C. M. Ko and P. Levai, Phys. Rev. C **68**, 034904 (2003); V. Greco, C. M. Ko and P. Levai, Phys. Rev. Lett. **90**, 202302 (2003); R. J. Fries, B. Muller, C. Nonaka and S. A. Bass, Phys. Rev. Lett. **90**, 202303 (2003).

7. D. Kharzeev, Phys. Lett. B **378**, 238 (1996); S. E. Vance, M. Gyulassy and X. N. Wang, Phys. Lett. B **443**, 45 (1998).
8. I. Vitev and M. Gyulassy, Nucl. Phys. A **715**, 779 (2003).
9. P. Huovinen, P. F. Kolb, U. W. Heinz, P. V. Ruuskanen and S. A. Voloshin, Phys. Lett. B **503**, 58 (2001).
10. M. Shao, O. Barannikova, X. Dong, Y. Fisyak, L. Ruan, P. Sorensen and Z. Xu, arXiv:nucl-ex/0505026.
11. E. Kistenev [PHENIX Collaboration], AIP Conf. Proc. **698**, 775 (2004).
12. M. Oldenburg [the STAR Collaboration], arXiv:nucl-ex/0510026.
13. H. Masui, arXiv:nucl-ex/0510018.
14. R. Baier, D. Schiff and B. G. Zakharov, Ann. Rev. Nucl. Part. Sci. **50**, 37 (2000); M. Gyulassy, I. Vitev, X. N. Wang and B. W. Zhang, arXiv:nucl-th/0302077.
15. D. Molnar, arXiv:nucl-th/0503051.
16. J. Adams *et al.* [STAR Collaboration], Phys. Rev. Lett. **95**, 122301 (2005).
17. V. Greco and C. M. Ko, Phys. Rev. C **70**, 024901 (2004).
18. B. Muller, R. J. Fries and S. A. Bass, Phys. Lett. B **618**, 77 (2005).
19. J. Adams *et al.* [STAR Collaboration], Phys. Lett. B **612**, 181 (2005); J. Adams *et al.* [STAR Collaboration], Phys. Rev. C **71**, 064902 (2005).
20. 0. Barannikova [STAR Collaboration], These proceedings.
21. J. Dunlop [STAR Collaboration], These proceedings.
22. S. S. Adler *et al.* [PHENIX Collaboration], Phys. Rev. C **69**, 034909 (2004).
23. M. Csanad [PHENIX Collaboration], arXiv:nucl-ex/0505001; M. Konno [PHENIX Collaboration], arXiv:nucl-ex/0510022; M. Shimomura, arXiv:nucl-ex/0510023.
24. A. Dainese, arXiv:nucl-ex/0510001; F. Antinori *et al.* [NA57 Collaboration], Phys. Lett. B **623**, 17 (2005).
25. S. Eidelman *et al.* [Particle Data Group], Phys. Lett. B **592**, 1 (2004).
26. R. L. Jaffe, Phys. Rev. D **15**, 267, 281 (1977); M. G. Alford and R. L. Jaffe, Nucl. Phys. B **578**, 367 (2000).
27. J. D. Weinstein and N. Isgur, Phys. Rev. D **41**, 2236 (1990); M. P. Locher, V. E. Markushin and H. Q. Zheng, Eur. Phys. J. C **4**, 317 (1998).
28. M. N. Achasov *et al.*, Phys. Lett. B **485**, 349 (2000); A. Aloisio *et al.* [KLOE Collaboration], Phys. Lett. B **537**, 21 (2002).
29. J. Adams *et al.* [STAR Collaboration], Phys. Rev. Lett. **92**, 092301 (2004).
30. H. Albrecht *et al.* [ARGUS Collaboration], Z. Phys. C **44**, 547 (1989).
31. A. Sickles [PHENIX collaboration], J. Phys. G **30**, S1291 (2004); S. S. Adler *et al.* [PHENIX Collaboration], Phys. Rev. C **71**, 051902 (2005).
32. J. Adams *et al.* [STAR Collaboration], arXiv:nucl-ex/0509030.
33. T. A. Trainor, arXiv:nucl-ex/0510035.
34. L. Ruan, arXiv:nucl-ex/0503018.